MOLECULAR DOCKING OF COUMARIN DERIVATIVES AS POTENTIAL DUAL-ACTION INHIBITOR FOR PROTEASE AND REVERSE TRANSCRIPTASE IN THE TREATMENT OF HIV/AIDS

Supported by tetfund TERTIARY EDUCATION TRUST FUND

Oluwakemi A. Oloba-Whenu* and Idris Olasupo

Department of Chemistry, University of Lagos, Nigeria
Corresponding Author: ooloba-whenu@unilag.edu.ng
Received: September 21, 2022 **Accepted:** November 12, 2022

Abstract

AIDS is one of the multifaceted diseases that develops from the infection of cells of the immune system by HIV virus, given room for severe opportunistic infections and this underlying complexity hampers its complete cure. Development of effective, safe and low-cost anti-HIV drugs is among the top global priority. Exploration of natural resources may give a ray of hope to develop new anti-HIV leads. HIV protease and reverse transcriptase inhibitors are one of the most important agents for the treatment of HIV infection. Coumarins have been reported to have various biological activities such as antiviral, antimicrobial anticancer. In this work molecular docking studies have been used to determine the binding of coumarin based derivatives as potential inhibitors of HIV-1 protease enzyme and reverse transcriptase enzyme. Molecular electrostatic potential and *in-silico* ADMET studies showed drug-likeness of these lead molecules. Molecular docking results show that the ligands bind very well in the active pocket of the enzymes with binding energy in the range -7.28 to -9.44 kcal/mol. The ILE50 and ASP 25 residues of the PR enzyme and the LYS101 residue of the RT enzyme played important roles in the binding of the coumarin to the enzymes. The calculated drug-like scores suggest these compounds have clinical potential and ADMET predictions point to acceptable pharmacokinetic and toxicity profiles.

NOTE: The abstract state clearly the method used and the findings and then conclude appropriately

Keywords: ADMET, Coumarin, HIV, molecular docking, protease, reverse transcriptase,

Introduction

Human immunodeficiency virus (HIV)/AIDS (Acquired Immunodeficiency Syndrome) pandemics remains a serious threat to health and development of mankind. In 2020, there were about 37.7 million people living with HIV, among which 10.2 million were not on HIV treatment. An estimated 1.5 million new HIV infections and 680,000 deaths from AIDS-related causes occurred(*UNAIDS data 2021*, 2021). Approved Anti-HIV drugs for therapeutic use are distributed into six categories based on their inhibitory mechanism and the various targets in the reproduction cycle of the virus: nucleoside reverse transcriptase inhibitors (NRTIs), non-nuleoside reverse transcriptase inhibitors (NNRTIs), protease inhibitors (PIs), integrase inhibitors (IIs), fusion inhibitors (FIs) and coreceptors antagonists (CAs)(Arts and Hazuda, 2012). Combination therapy using the above classes of inhibitors commonly called HAART (Highly active antiretroviral therapy) remains the most common treatment protocol(Tukulula, Klein and Kaye, 2010) thus improving life expectancy. However, the HAART approach is expensive, often not well tolerated and patient's non-compliance lead to multidrug resistant strains. An alternative approach attracting increasing number of researches is the design of dual inhibitors(Olomola *et al.*, 2013). It is well known that both reverse transcriptase (RT) and Protease (PR) enzymes play key roles in viral replication. RT, a HIV enzyme necessary to catalyze the conversion of viral RNA into DNA, which on entering the host cell nucleus will be integrated into the genetic material of the host(Zhu *et al.*, 2021), while protease, cleaves the gag and gag-pol polyproteins required by the infectious virus to mature. Inhibition of the HIV RT and/or PR slow or results in immature virons that are incapable of replication(Su, Koh and Gan, 2019) therefore a search for natural materials capable of such suppression has become desirable

Coumarin, a biologically active natural product has attracted attention in recent years due to its diverse pharmacological properties. An oxygen-containing heterocycle (2H-chromen-2-ones or 2H-1-benzopyran-2-ones) derivatives are considered as a privileged structure for designing novel agents having high affinity and specificity to different molecular targets(Hassan *et al.*, 2016) and endowed with a unique characteristic pharmacophore of planar aromatic nucleus connected with a hydrogen bond acceptor; lactone group as a facilitator of protein ligand binding for antiviral agents (Torres *et al.*, 2014). Coumarins have been reported to exhibit valuable biological activities among which are: anticoagulant(Kasperkiewicz *et al.*, 2020), anticancer(Salem *et al.*, 2018), antioxidant(Randive *et al.*, 2015), anti-inflammatory agents(Thomas *et al.*, 2017), HIV inhibitor(Olomola, Kaye and Klein, 2014) and anti-diabetic(Soni *et al.*, 2019) among others.

As part of the group's research focus: application of Baylis-Hillman methodology in the construction of heterocyclic compounds as potential HIV inhibitors, we have in the past reported the synthesis of benzyl ether based β-amino-β-hydroxyl esters (aza-Michael compounds) of Salicyaldehyde(Olasupo, Adams and Familoni, 2018). Molecular docking is an efficient way to investigate non-covalent bonding interaction between macromolecules and small molecules We hereby report the progress, in the area of application, on the earlier work on design and synthesis

of Baylis-Hillman-derived coumarin derivatives(Olasupo *et al.*, 2014), as dual-action HIV-1 protease/reverse transcriptase (PR/RT) inhibitors. The electronic structure and physicochemical properties of the coumarin are also reported

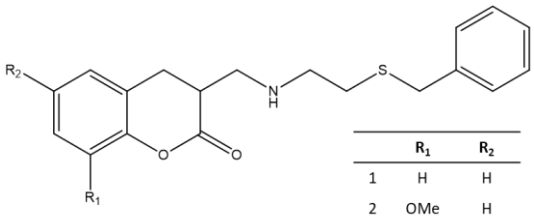

	R_1	R_2
1	H	H
2	OMe	H
3	OEt	H
4	H	Br

Computational details

Initial conformational search of coumarin derivatives was performed on each analogue using Avogadro software (Hanwell *et al.*, 2012) http://avogadro.cc/ and the MMFF 94 force field(Halgren, 1996), molecular mechanics model; the ten lowest energy conformers were further optimized at the B3PW91/6-31G (d,p) level of theory using Gaussian 09W(Gaussian 09, Revision D.01; Frisch, *et al.* 2009) and frequency calculations were also carried out to confirm the nature of stationary point at the same level of theory. The GaussView(Dennington, Keith and Millam, 2009) software was used to generate the optimized structures. Gaussian 09W. Electronic analysis of the lowest conformer after DFT optimization, is reported at this level of theory and was used for the molecular docking analysis.

Molecular docking to determine the binding modes and inhibition potential was carried out using the AutoDock 4.2 software(Morris *et al.*, 2009; Forli *et al.*, 2016). Molecular docking relies on the use of force field to estimate the free binding energy of the protein-ligand complex. The crystal structure of the enzymes were obtained from the protein data bank (https://www.rcsb.org/pdb)(Berman *et al.*, 2000); the HIV-1 RT in complex with rilpivirine (TMC278, Edurant), a non-nucleoside rt-inhibiting drug pdbid 4g1q,(Kuroda *et al.*, 2013) with resolution: 1.51 Å and the HIV-1 PR complexed with xv638 of dupont pharmaceuticals, pdbid 1bwa(Ala *et al.*, 1998) with resolution: 1.90 Å. The protein targets were subjected to pre –docking preparation using the discovery studio software (http://www.accelrys.com) to remove the water molecules and bound ligands and the AutoDockTools (ADT)(Morris *et al.*, 2009) was used to add polar hydrogen atoms as they are absent from the crystallographic structure sourced from the protein data bank and geister charges. Based on the bound ligands, the coordinate of the active pocket of the enzymes were determined using LigPlot+(Laskowski and Swindells, 2011) as obtained from pdbsum webpage(www.ebi.ac.uk/pdbsum). The Autogrid program within the Autodcok 4.2 was used to set up a grid map, centered at 42.73 × 34.085 × 39.395 Å for the protease enzyme while for the reverse transcriptase, the grid box was centred at 51.665 × -28.333 × 30.662 Å. For both enzymes, the box size is 60 × 60 × 60 Å and the grid spacing was 0.375 Å. The lamarckian genetic algorithm was used to find the docking poses. Autodocktools and the discovery studio software were used to visualize the docking results. Each ligand was analysed for receptor binding energy, inhibition constant and interactions present. The pharmacological properties of the coumarin derivatives were explored using the swissadme online tool(Daina, Michielin and Zoete, 2017) (http://www.swissadme.ch/index.php). The FDA approved drugs, Delavirdin and Darunavir, were used as benchmark for analysis of efficacies of the coumarins on the inhibition of reverse transcriptase and protease transcriptase enzyme respectively.

NOTE: The method used in this study should be stated clearly

Results

DFT studies

The optimized structures of the most stable conformer of the coumarin derivatives being considered as dual inhibitor for HIV-1 protease and reverse transcriptase enzymes are displayed in Figure 1. The electron density plots for the lowest unoccupied molecular orbital (LUMO), highest occupied molecular orbitals (HOMO) and electrostatic potential maps are also given. Table 1 gives the calculated molecular descriptors obtained from the energies of the HOMO and LUMO. Generally, the HOMOs are centered on the thiobenzyl and the two of the heteroatoms, nitrogen and sulphur for **1** and **4**, on the pyrone moiety for **2** and over the entire molecule for **3**. while the LUMOs are centered on the pyrone part of the coumarin derivatives in all cases which suggests a possibility of charge transfer within the molecule.

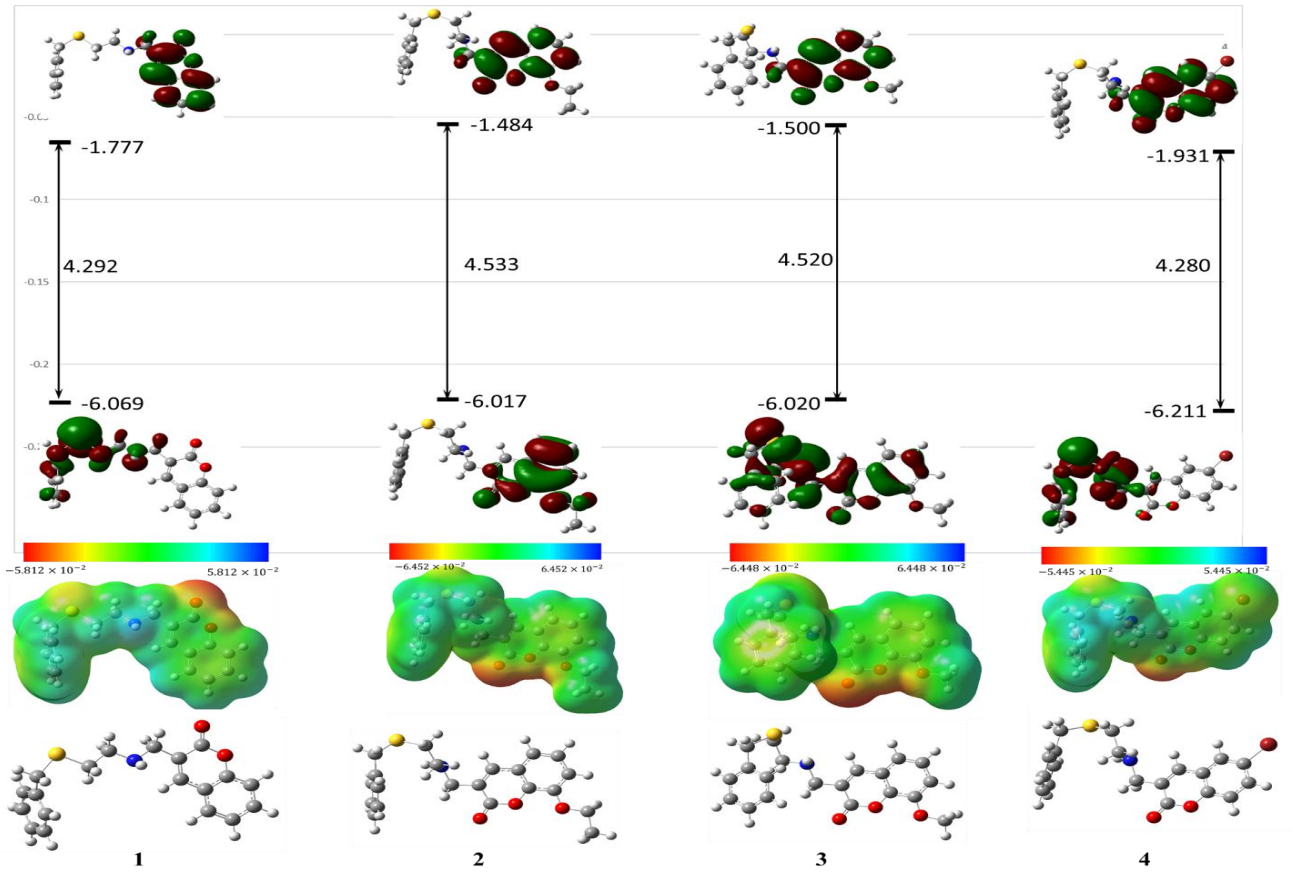

Figure 1: Optimized structure, HOMO, LUMO and ESP of the comarine derivatives

Table 1: The electronic properties of the binding modes of the ligand conformers showing the HOMO energy, E_{HOMO}, LUMO energy,E_{LUMO}, absolute HOMO-LUMO gap energies,ΔE_{gap}, molecular descriptors and the dipole moment.

Cou.	E_{HOMO}, (eV)	E_{LUMO}, (eV)	ΔE_{gap}, (eV)	$I(eV)$	$A(eV)$	$\eta,(eV)$	μ, (eV)	χ, (eV)	ω, (eV)	S, (eV)	**D.M**
1	-6.069	-1.777	4.292	6.069	1.777	2.146	3.923	-3.923	16.51	0.233	5.3
2	-6.017	-1.484	4.533	6.017	1.484	2.267	3.751	-3.751	15.94	0.221	3.2
3	-6.020	-1.500	4.520	6.020	1.500	2.260	3.760	-3.760	15.97	0.221	2.4
4	-6.211	-1.931	4.280	6.211	1.931	2.140	4.071	-4.071	17.73	0.234	2.5

Key: Chemical hardness: $\eta,(eV)$; Ionization potential: I, (eV); Chemical potential: μ, (eV); Electronegativity: χ, (eV); Global softness: S, (eV); $\Delta E_{gap} = E_{LUMO} - E_{HOMO},(eV)$; electrophilicity index: ω, (eV) D.M: dipole moment; electron affinity $A(eV)$

Molecular docking studies

All four ligands were observed to bind perfectly in the active pocket of both enzyme targets and the docking studies revealed a high affinity between the target protein and the four coumarin ligands. The 2D and 3D ligand interaction of the coumarin ligands with the protease enzyme are displayed in Figure 2. The molecular docking results, binding energies(BE), inhibition constant (K) and interactions between ligands and enzymes, are summarized in Tables 2 and 3 respectively for the protease and reverse transcriptase enzymes. With the protease enzyme, the observed binding energies observed with ligands **1**, **2**, **3, 4** and darunavir respectively are -8.85, -7.28 -8.53 -9.33 and -8.98kcal/mol; and the inhibition constants are 327.141, 4.61, 555.13, 144.27 and 263.34nM. Hydrogen bonding plays a significant role in bonding stability between drug target and ligands with approved distance less than 3.5 Å. From ADT and DS analysis, the conventional hydrogen bond was observed with ILE 50A (chain A) and the carbonyl (C=O) bond on the pyrone moiety with bond distance in the range 2.14 to 2.22 Å; between ILE 50B and oxygen atom in the ring with hydrogen bond distance in the range 1.70 to 2.07 Å and between ASP 25B and hydrogen atom of the N-H group with hydrogen bond distance in the range 1.68 to 2.16 Å in all

cases all of which have hydrogen bond distances ranging from 1.8 to 2.2Å. Other types of interactions present between protease and all the ligands considered are the π -alky interaction between the pyrone ring and VAL 84 and between the benzene ring of the thiobenzyl moiety and the ALA 28 and ILE 47 amino acid residues on chain A; amide-π stacked interaction between benzene ring and GLY 49 observed in **1;** alkyl interaction, carbon-hydrogen π -donor hydrogen bond and as expected van der Waals interactions in different extents. The bromide atom presents in **4** is also involved in with π-alkyl interaction with PHE 82 and LEU 23 both on chain A

The corresponding binding energies between the ligands and the reverse transcriptase enzyme are -8.12, -8.55, -7.58 -9.44 and -8.43kcal/mol and inhibition constant 1.11, 537.8, 2.81, 86.64 and 663 nM respectively for **1**, **2**, **3 4** and delavirdine. All four ligands are in hydrogen bonding with the LYS 101 amino acid residue and π-π interaction with the TYR 318 residue. The observed hydrogen bonds are between LYS 101 and the carbonyl oxygen, bond distance 1.71 to 1.97 Å; and between the same amino acid residue LYS 101 and hydrogen atom of the NH group, 1.92 to 2.15 Å. Additional hydrogen bond is observed in **2** and **3** between LYS 101 and the alkoxy group, 1.88 to 2.06 Å. There is a π-stacked interaction between the thiazole ring and the aromatic TYR 318 residue and π-sulphur interaction between the Sulphur atom and the PHE 227 amino acid. Additional interactions present are carbon-hydrogen bond, pi-sigma, pi-sulphur, pi-alkyl, π-π T shaped interaction.

Table 2: Binding free energies and inhibition constants of the best binding modes from docking Simulation of each coumarin derivative with the HIV-1 protease enzyme pdbid:1bwa

Ligand	No of H-bonds	Interacting Aminoacid	Binding Energy (kcal/mol)	Inhibition Constant (nM)	Other interactions
1	3	ILE50, ILE 50, ASP 25	-8.85	327.41	Amide-π stacked, π-alkyl, carbon-hydrogen, van der Waal
2	3	ILE50, ILE 50, ASP 25	-7.28	4.61	π-donor hydrogen bond, π-alkyl, carbon-hydrogen, van der Waal
3	3	ILE50, ILE 50, ASP 25	-8.53	555.13	alkyl, π-alkyl, carbon-hydrogen, van der Waal
4	3	ILE50, ILE 50, ASP 25	-9.33	144.27	π-donor hydrogen bond, π-alkyl, alkyl, van der Waal
Dar.	3	ASP 25, ILE 50, THR 80	-8.98	263.34	π-sigma, Amide-π stacked, alkyl, π-alkyl

Dar.: darunavir

Table 3: Binding free energies and inhibition constants of the best binding modes from docking simulation of each coumarin derivative with the HIV-1 reverse transcriptase enzyme, pdbid:4g1q

Ligand	No of H bonds	Interacting Aminoacid	Binding energy (kcal/mol)	Inhibition Constant (nM)	Other interactions
1	2	LYS 101	-8.12	1.11	carbon-hydrogen, π-sigma, π-alkyl, π-sulphur
2	3	LYS 101	-8.55	537.8	carbon-hydrogen, π-sigma, π-alkyl, π-sulphur π-π stacked, π-π-T-shaped,
3	3	LYS 101	-7.58	2.81	carbon-hydrogen, π-sigma, π-sulphur, π-π-T-shaped, alkyl, π-alkyl,
4	2	LYS 101	-9.44	86.64	carbon-hydrogen, π-sigma, π-alkyl, π-sulphur
Del.	2	LYS 101	-8.43	663	π-cation, π-donor hydrogen bond, π-sigma, π-π stacked, alkyl, π-alkyl,

Del.: delavirdine

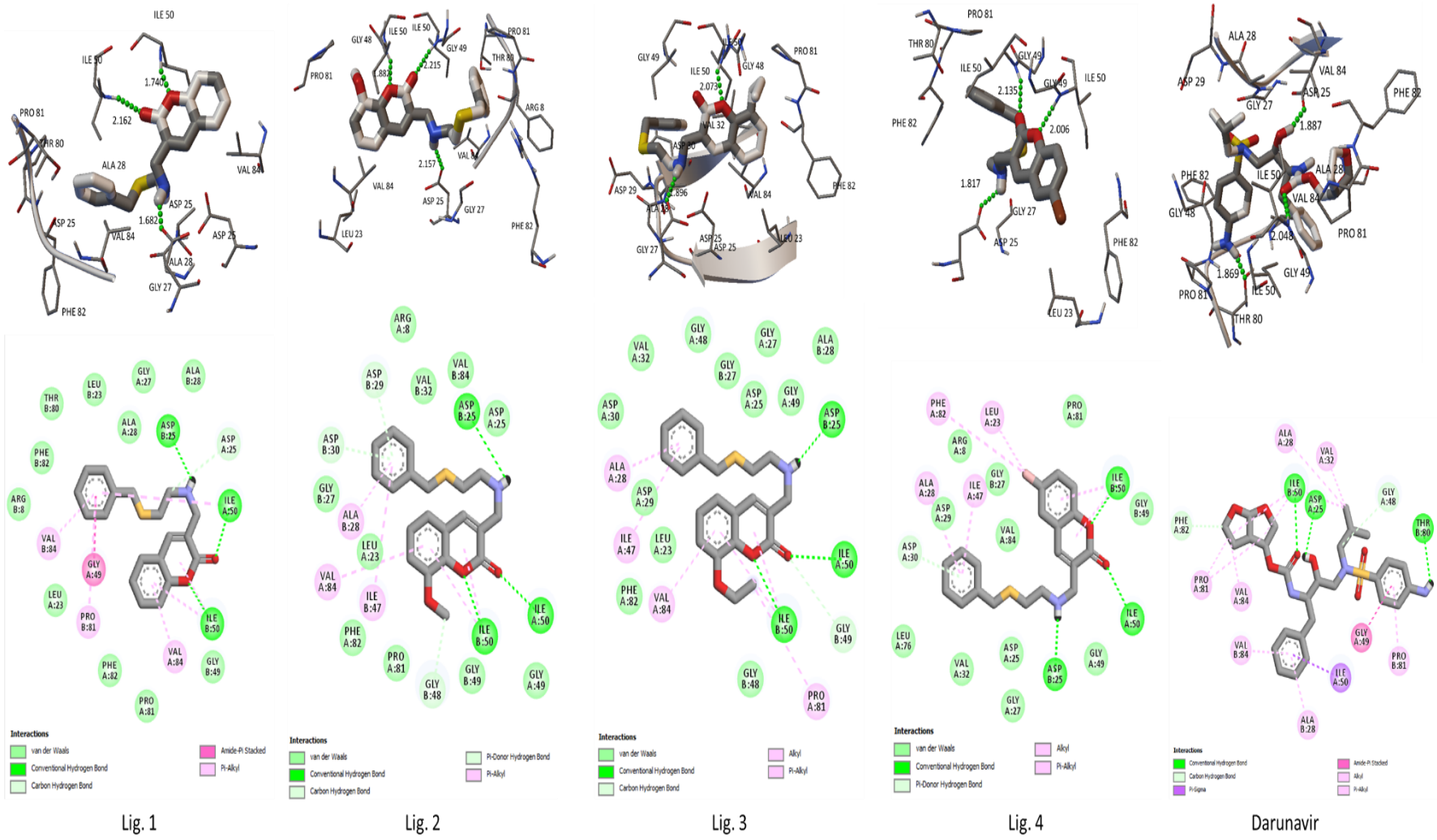

Figure 2: the 3D and 2D representation of the docked pose of the coumarin ligands in the active pocket of the protease enzyme.. H-bond, alkyl-π, and sigma-π interactions are represented by green, pink, and violet dotted lines respectively

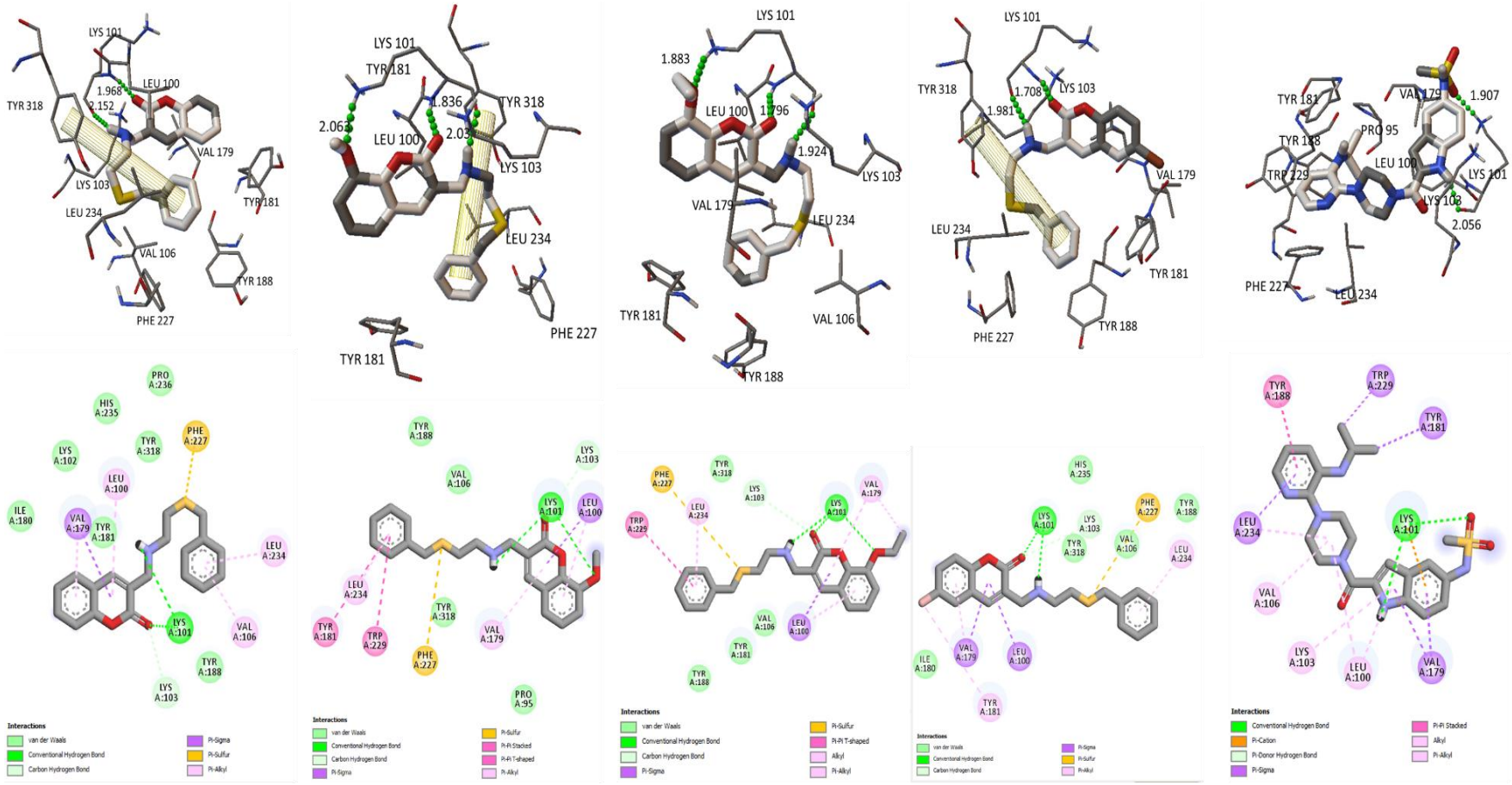

Figure 3: 3D and 2D representation of the docked poses of the coumarin ligands 1, 2, 3 and 4 in the binding pocket of the reverse transcriptase enzyme. H-bond, alkyl-π, and sigma-π interactions are represented by green, pink, and violet dotted lines respectively

ADMET studies

All four compounds and respective standards were screened for druglikeliness in the swissadme server and the results are given in Table 4.

Table 4: Predicted absorption-distribution-metabolism- excretion (ADME) parameters and drug-like properties of the four coumarin derivatives, delavirdine and darunavir

Property	Parameters	1	2	3	4	Delavirdine	Darunavir
Physico-chemical Properties	MW	325.42	355.45	369.48	404.32	456.56	547.66
	#Rotatable bonds	7	8	9	7	7	13
	#H-bond acceptors	3	4	4	3	4	8
	#H-bond donors	1	1	1	1	3	3
	MR	96.75	103.24	108.05	104.45	134.45	142.2
	TPSA	67.54	76.77	76.77	67.54	118.81	148.8
Lipo-philicity	iLOGP	3.1	3.43	3.85	3.73	2.55	3.2
	XLOGP3	3.98	3.95	4.32	4.67	2.45	2.94
	WLOGP	3.51	3.52	3.91	4.27	2.65	3.46
	MLOGP	3.17	2.81	3.04	3.78	0.75	1.18
	Consensus Log P	3.71	3.71	4.07	4.38	1.94	2.45
Water Solubility	ESOL Class	MS	MS	MS	MS	MS	MS
	Ali Class	MS	MS	MS	MS	MS	MS
	Silicos-IT class	PS	PS	PS	PS	PS	MS
Pharmaco-kinetics	GI absorption	High	High	High	High	High	Low
	BBB permeant	Yes	Yes	Yes	Yes	Yes	No
Drug-likeness	Lipinski violations	0	0	0	0	0	1
	Ghose violations	0	0	0	0	1	3
	Veber violations	0	0	0	0	0	2
	Egan violations	0	0	0	0	0	1
	Muegge violations	0	0	0	0	0	0
	Bioavailability Score	0.55	0.55	0.55	0.55	0.55	0.55
Medicinal Chemistry	PAINS alerts	0	0	0	0	0	0
	Brenk #alerts	1	1	1	1	0	1
	Leadlikeness violations	1	3	3	2	1	2
	Synthetic Accessibility	3.33	3.48	3.55	3.33	3.33	5.67

*MS=moderately soluble; PS=poorly soluble

Discussions

The energy difference between these two orbitals can be used to explain the chemical behavior of the molecule. The wider the HOMO-LUMO range in a molecule, the more stable the molecule, and vice versa. Analysis of the ΔE_{gap} indicates that the values are small and relatively of similar values in the range 4.280 – 4.533 and increases in the order **4** ≈**1** < **3** ≈ **2** i.e. the presence of the alkoxy group in **2 (**OEt**)**

and **3** (OMe) widens the HOMO-LUMO gap slightly. A small ΔE_{gap} is characteristic of highly conjugated π-systems. The energy of the HOMO and LUMO can also be used to determine the chemical properties such as ionization potential, electron affinity, chemical potential, electronegativity, chemical hardness, chemical softness, electrophilicity(Jensen, 2017). The calculated values of these descriptors are reported in Table 1. The ionization potential is the minimum energy required to remove an electron from the molecule; the ease of removing electron follows the order **2** > **3** > **1** > **4.** Electron affinity is defined as the increases in the amount of energy when an electron is added to molecule and follows the trend **2** ≈ **3** < **1** < **4**. Electronegativity refers to the measure of the molecule ability to attract electrons and follows the order **4** > **1** > **3** ≈ **2**, with **4** having the highest force of attraction. Chemical hardness is a measure of charge transfer inhibition within the molecule, and molecules with high chemical hardness value have little or no charge transfer within the molecule. Simply, hard molecules have a high resistance to changing their electronic distribution during a reaction, whereas soft molecules have a low resistance to changing their electronic distribution during a reaction. Table 1 also shows chemical hardness trend of 2 ≈ 3 > 1 ≈ 4, reflecting the structural similarities of the molecules and the contribution of the alkoxy groups to their relative chemical activities. Electrophilicity (ω) is a predictor for the electrophilic nature of a chemical species; it measures the propensity of molecule to accept an electron, with high values of ω characterizing good electrophilicity in a molecule. The ranking of organic molecules on electrophilicity scale classifies as weak electrophiles those with ω less than 0.8 eV, moderate electrophiles have ω in a range between 0.8 and 1.5 eV, and strong electrophiles have ω greater than 1.5 eV(Edim *et al.*, 2021). The calculated values show that the coumarins are strong electrophiles. All the above descriptors have been defined in the gaseous phase(Pearson, 1986, 1987; Reed, 1997; Parr, Szentpály and Liu, 1999).

The molecular electrostatic potential (MEP) generated in space around a molecule by the charge distribution is useful to comprehend electrophilic or nucleophilic properties and provides information regarding the chemical reactivity of a molecule represented by various colours. The negative molecular electrostatic potential is in shades of red and resembles an attraction of proton by electron density in the molecule, the positive electrostatic potential represented by shades of blue corresponds to the attraction of electron density to the molecule; green represents regions of zero potential. From Figure 1, the negative electrostatic potential spread over the oxygen atoms in the pyrone moiety and the positive electrostatic potential concentrates over the hydrogen atom of the N-H bond. Thus, the H atom is the most reactive site for nucleophilic attack while the pyrrole moiety acts as the center for electrophilic attack. The presence of the alkoxy group in **2** and **3** diffuses the nucleophilic region.

Molecular docking of the coumarin derivatives were performed to ascertain the inhibition potentials of the ligands on HIV-1 protease and reverse transcriptase. For the protease enzyme, a 22 kDa homodimer, with each subunit made up of 99 amino acids, the active pocket lies between the identical subunits and has the characteristic Asp-Thr-Gly (Asp25, Thr26 and Gly27) catalytic triad sequence common to aspartic proteases located in-between both chains A and B in accordance with the reported binding sites in literature of some ligands to HIV-1 protease(Brik and Wong, 2003). The active residues responsible for hydrogen bonding interactions are Asp25, Gly27, Gly48 and Ile50 (of both chains). and have good interaction with the amino acids present for the activity of the enzymes. The lower the binding energy the higher the binding affinity, docking studies also showed that **4** gave the most negative binding energy of -9.33 kcal/mol. The licensed protease inhibitors are Saquinavir, Ritonavir, Indinavir, Nelfinavir, Amprenavir, Lopinavir, Atzanavir, Tipranavir and Darunavir etc. As of 2016, Darunavir is an Office of AIDS Research Advisory Council (OARAC) recommended treatment option. Therefore, Darunavir was taken as a standard protease inhibitor. The binding energy of -8.98 kcal/mol observed with darunavir is not as low as what was observed with **4** and relatively comparable with BE of **1** and **3** but lower than the BE of **2.** The inhibition constant 263.34 nM is higher than the K of all ligands except for **1**. The presence of OEt and OMe group in **2** and **3** respectively did not seem to afford additional hydrogen bond interaction, it rather seems to elongate the H-bond between ILE50B with the oxygen atom embedded in the ring. However, the bromide atom presents in **4** is involved in with π-alkyl interaction with PHE 82 and LEU 23 both residues on chain A

Similar to the what was observed with the protease enzyme, all four ligands fit perfectly in the binding pocket of the reverse transcriptase enzyme. Unlike with the protease enzyme, the alkoxy group provides additional inhibition with the reverse transcriptase. Emtricitabine, Didanosine, Abacavir and Lamivudine, Efavirenz, Etravirine, Delavirdine are some of the widely used reverse transcriptase inhibitors. Delavirdine was selected as the standard because it is the latest and commonly used drug for this target. The calculated binding energy between delavirdine and the reverse transcriptase 4g1q is -8.43 kcal/mol of which the coumarin derivatives have comparable values. The inhibition constant is 663 nM which is considerably higher than the inhibition constant calculated for the coumarins except for **2**.

Chemical absorption, distribution, metabolism, excretion, and toxicity (ADMET) properties play a crucial role in determining the drug-likeliness of organic molecules in order to become a successful drug candidate. Swissadme server screens for various descriptors for drug-likeliness which includes but not limited to molecular weight (MW), molecular refractivity (MR), topological polar surface area (TPSA), *n*-octanol and water (log $P_{o/w}$) which are the classical descriptor for *Lipophilicity*, *Water Solubility*, human gastrointestinal absorption (HIA) and blood-brain barrier (BBB) permeation(Daina, Michielin and Zoete, 2014, 2017; Daina and Zoete, 2016). While these descriptors are not accurate enough to replace the in vivo or in vitro assay, they can help point out expected physicochemical properties and suggest if optimizations are required

thereafter. A potential drug against a biological target must align with several properties such as the Lipinski rule of five which are: no more than 5 hydrogen bond donors, no more than 10 hydrogen bond acceptors, all nitrogen or oxygen atoms, a molecular mass less than 500 daltons, an octanol-water partition coefficient (log P) that does not exceed 5(Lipinski *et al.*, 2001). According to these results, it is observed that all four coumarin derivatives passed the Lipinski rule of 5 and the other druglikeliness measures which are Ghose(Ghose, Viswanadhan and Wendoloski, 1999), Veber(Veber *et al.*, 2002), Egan(Egan, Merz and Baldwin, 2000) or Muegge(Muegge, Heald and Brittelli, 2001). Since the molecules do not violate these rukes, they are deemed bioavailable. Also, it is noted that our coumarin derivatives were predicted to have a high gastrointestinal absorption and blood-brain barrier (BBB) permeation, Table 4, indicating that the drugs will reach target destination. The topological polar surface area (TPSA) values were in the range from 67.5 to 96.8 $Å^2$, which suggested that they will possess good transport properties *in vivo*. Also, it is observed that the synthetic accessibilities of designed compounds were lower than 5, suggesting that they are relatively easy to be synthesized. Water Solubility was modeled by ESOL model (Delaney, 2004), Ali model (Ali *et al.*, 2012) and the SILICOS-IT (Daina, Michielin and Zoete, 2017); the molecules are poorly to moderately soluble in water. Compared to the current drugs, the ADME properties of the four coumarin derivatives compounds were superior. Thus, the four newly designed coumarin derivatives might be said to have good pharmacokinetics properties.

Conclusion and further discussion

The HIV-1 PR and RT enzymes are part of the most important target to inhibit the development of HIV to AIDS disease. Coumarin and coumarin-related compounds have proven for many years to have significant therapeutic potential. The coumarins are of great interest, due to their biological properties. Their physiological, bacteriostatic and anti-tumour activities make these compounds attractive for further backbone derivatisation and screening as novel therapeutic agents. Molecular docking, using Autodock4.0 which uses the Lamarckian genetic algorithm (LGA), DFT descriptors and ADMET properties was reported for the four coumarin derivatives.

MEP distribution revealed the potential sites of electrophilic and nucleopholic attack as the delocalized region containing the oxygen atoms and N-H regions respectively. ADMET profile of the coumarins as good candidates for lead optimization as none violated the drug-likeliness rules: Lipinski's rule of 5, Ghose, Veber, Egan and Muegge while the BBB permeation is also of good value. Molecular docking shows that the compounds have good biological activity towards the two enzymes PR and RT. The presence of the aromatic residues afforded more interactions in the RT than in the PR enzyme. The derivative **4** gave the least binding energy with both enzymes with binding energy values -9.33 and -9.44 kcal/mol respectively with PR and RT, thus making it best probable lead drug candidate.

References

Ala, P.J. *et al.* (1998) 'Counteracting HIV-1 Protease Drug Resistance: Structural Analysis of Mutant Proteases Complexed with XV638 and SD146, Cyclic Urea Amides with Broad Specificities', *Biochemistry*, 37(43), pp. 15042–15049. Available at: https://doi.org/10.1021/bi980386e.

Ali, J. *et al.* (2012) 'Revisiting the general solubility equation: In silico prediction of aqueous solubility incorporating the effect of topographical polar surface area', *Journal of Chemical Information and Modeling*, 52(2), pp. 420–428. Available at: https://doi.org/10.1021/ci200387c.

Arts, E.J. and Hazuda, D.J. (2012) 'HIV-1 antiretroviral drug therapy', *Cold Spring Harbor perspectives in medicine*, 2(4), pp. a007161–a007161. Available at: https://doi.org/10.1101/cshperspect.a007161.

Berman, H.M. *et al.* (2000) 'The Protein Data Bank', *Nucleic Acids Research*, 28(1), pp. 235–242. Available at: https://doi.org/10.1093/nar/28.1.235.

Brik, A. and Wong, C.H. (2003) 'HIV-1 protease: Mechanism and drug discovery', *Organic and Biomolecular Chemistry*, 1(1), pp. 5–14. Available at: https://doi.org/10.1039/b208248a.

Daina, A., Michielin, O. and Zoete, V. (2014) 'iLOGP: A Simple, Robust, and Efficient Description of n-Octanol/Water Partition Coefficient for Drug Design Using the GB/SA Approach', *Journal of Chemical Information and Modeling*, 54(12), pp. 3284–3301. Available at: https://doi.org/10.1021/ci500467k.

Daina, A., Michielin, O. and Zoete, V. (2017) 'SwissADME: a free web tool to evaluate pharmacokinetics, drug-likeness and medicinal chemistry friendliness of small molecules', *Scientific Reports*, 7(1), p. 42717. Available at: https://doi.org/10.1038/srep42717.

Daina, A. and Zoete, V. (2016) 'A BOILED-Egg To Predict Gastrointestinal Absorption and Brain Penetration of Small Molecules', *ChemMedChem*, 11(11), pp. 1117–1121. Available at: https://doi.org/https://doi.org/10.1002/cmdc.201600182.

Delaney, J.S. (2004) 'ESOL: Estimating aqueous solubility directly from molecular structure', *Journal of Chemical Information and Computer Sciences*, 44(3), pp. 1000–1005. Available at: https://doi.org/10.1021/ci034243x.

Dennington, R., Keith, T. and Millam, J. (2009) 'GaussView, Version 5.', *Semichem Inc.* , *Shawnee Mission, KS*, p. Semichem Inc.

Edim, M.M. *et al.* (2021) 'Aromaticity indices, electronic structural properties, and fuzzy atomic space

investigations of naphthalene and its aza-derivatives', *Heliyon*, 7(2), p. e06138. Available at: https://doi.org/https://doi.org/10.1016/j.heliyon.2021.e06138.

Egan, W.J., Merz, K.M. and Baldwin, J.J. (2000) 'Prediction of drug absorption using multivariate statistics', *Journal of Medicinal Chemistry*, 43(21), pp. 3867–3877. Available at: https://doi.org/10.1021/jm000292e.

Forli, S. *et al.* (2016) 'Computational protein–ligand docking and virtual drug screening with the AutoDock suite', *Nature Protocols*, 11(5), pp. 905–919. Available at: https://doi.org/10.1038/nprot.2016.051.

Frisch, M. J.; Trucks, G. W.; Schlegel, H. B.; Scuseria, G. E.; Robb, M. A.; Cheeseman, J. R.; Scalmani, G.; Barone, V.; Mennucci, B.; Petersson, G. A.; Nakatsuji, H.; Caricato, M.; Li, X.; Hratchian, H. P.; Izmaylov, A. F.; Bloino, J.; Zheng, G.; Sonnenberg, J. L.; Hada, M.; Ehara, M.; Toyota, K.; Fukuda, R.; Hasegawa, J.; Ishida, M.; Nakajima, T.; Honda, Y.; Kitao, O.; Nakai, H.; Vreven, T.; Montgomery, J. A., Jr.; Peralta, J. E.; Ogliaro, F.; Bearpark, M.; Heyd, J. J.; Brothers, E.; Kudin, K. N.; Staroverov, V. N.; Kobayashi, R.; Normand, J.; Raghavachari, K.; Rendell, A.; Burant, J. C.; Iyengar, S. S.; Tomasi, J.; Cossi, M.; Rega, N.; Millam, J. M.; Klene, M.; Knox, J. E.; Cross, J. B.; Bakken, V.; Adamo, C.; Jaramillo, J.; Gomperts, R.; Stratmann, R. E.; Yazyev, O.; Austin, A. J.; Cammi, R.; Pomelli, C.; Ochterski, J. W.; Martin, R. L.; Morokuma, K.; Zakrzewski, V. G.; Voth, G. A.; Salvador, P.; Dannenberg, J. J.; Dapprich, S.; Daniels, A. D.; Farkas, Ö.; Foresman, J. B.; Ortiz, J. V.; Cioslowski, J.; Fox, D. J. Gaussian, Inc., Wallingford CT, (2009) Gaussian 09, Revision D.01; Available at: http://gaussian.com/.

Ghose, A.K., Viswanadhan, V.N. and Wendoloski, J.J. (1999) 'A knowledge-based approach in designing combinatorial or medicinal chemistry libraries for drug discovery. 1. A qualitative and quantitative characterization of known drug databases', *Journal of Combinatorial Chemistry*, 1(1), pp. 55–68. Available at: https://doi.org/10.1021/cc9800071.

Halgren, T.A. (1996) 'Merck molecular force field. I. Basis, form, scope, parameterization, and performance of MMFF94', *Journal of Computational Chemistry*, 17(5–6), pp. 490–519. Available at: https://doi.org/https://doi.org/10.1002/(SICI)1096-987X(199604)17:5/6<490::AID-JCC1>3.0.CO;2-P.

Hanwell, M.D. *et al.* (2012) 'Avogadro: an advanced semantic chemical editor, visualization, and analysis platform', *Journal of Cheminformatics*, 4(1), p. 17. Available at: https://doi.org/10.1186/1758-2946-4-17.

Hassan, M.Z. *et al.* (2016) 'Therapeutic potential of coumarins as antiviral agents', *European Journal of Medicinal Chemistry*, 123, pp. 236–255. Available at: https://doi.org/10.1016/j.ejmech.2016.07.056.

Jensen, F. (2017) *Introduction to Computational Chemistry*. Wiley. Available at: https://books.google.com.ng/books?id=UZOVDQAAQBAJ.

Kasperkiewicz, K. *et al.* (2020) 'Antagonists of Vitamin K-Popular Coumarin Drugs and New Synthetic and Natural Coumarin Derivatives', *Molecules (Basel, Switzerland)*, 25(6), p. 1465. Available at: https://doi.org/10.3390/molecules25061465.

Kuroda, D.G. *et al.* (2013) 'Snapshot of the equilibrium dynamics of a drug bound to HIV-1 reverse transcriptase', *Nature Chemistry*, 5(3), pp. 174–181. Available at: https://doi.org/10.1038/nchem.1559.

Laskowski, R.A. and Swindells, M.B. (2011) 'LigPlot+: Multiple Ligand–Protein Interaction Diagrams for Drug Discovery', *Journal of Chemical Information and Modeling*, 51(10), pp. 2778–2786. Available at: https://doi.org/10.1021/ci200227u.

Lipinski, C.A. *et al.* (2001) 'Experimental and computational approaches to estimate solubility and permeability in drug discovery and development settings.', *Advanced drug delivery reviews*, 46(1–3), pp. 3–26. Available at: https://doi.org/10.1016/s0169-409x(00)00129-0.

Morris, G.M. *et al.* (2009) 'AutoDock4 and AutoDockTools4: Automated docking with selective receptor flexibility', *Journal of Computational Chemistry*, 30(16), pp. 2785–2791. Available at: https://doi.org/https://doi.org/10.1002/jcc.21256.

Muegge, I., Heald, S.L. and Brittelli, D. (2001) 'Simple selection criteria for drug-like chemical matter', *Journal of Medicinal Chemistry*, 44(12), pp. 1841–1846. Available at: https://doi.org/10.1021/jm015507e.

Olasupo, I. *et al.* (2014) 'Evaluation of Baylis–Hillman Routes to 3-(Aminomethyl)coumarin Derivatives', *Synthetic Communications*, 44(2), pp. 251–258. Available at: https://doi.org/10.1080/00397911.2013.803575.

Olasupo, I.A., Adams, L. and Familoni, O.B. (2018) 'Synthesis and Molecular Docking Studies of Benzyl Protected Aza-Michael Products of Salicyaldehyde', *Centrepoint Journal*, 24(1), pp.

161–196.

Olomola, T.O. *et al.* (2013) 'Synthesis and evaluation of coumarin derivatives as potential dual-action HIV-1 protease and reverse transcriptase inhibitors.', *Bioorganic & medicinal chemistry*, 21(7), pp. 1964–1971. Available at: https://doi.org/10.1016/j.bmc.2013.01.025.

Olomola, T.O., Kaye, P.T. and Klein, R. (2014) 'Synthesis of cinnamate ester "AZT conjugates as potential dual-action HIV-1 integrase and reverse transcriptase inhibitors', *Tetrahedron*. Elsevier Ltd.

Parr, R.G., Szentpály, L. V. and Liu, S. (1999) 'Electrophilicity index', *Journal of the American Chemical Society*, 121(9), pp. 1922–1924. Available at: https://doi.org/10.1021/ja983494x.

Pearson, R.G. (1986) 'Absolute electronegativity and hardness correlated with molecular orbital theory', *Proceedings of the National Academy of Sciences*, 83(22), pp. 8440–8441. Available at: https://doi.org/10.1073/pnas.83.22.8440.

Pearson, R.G. (1987) 'Recent advances in the concept of hard and soft acids and bases', *Journal of Chemical Education*, 64(7), pp. 561–567. Available at: https://doi.org/10.1021/ed064p561.

Randive, K.H. *et al.* (2015) 'Synthesis and Biological Evaluation of Novel Coumarin Derivatives as Antioxidant Agents', *Bioorganicheskaia khimiia*, 41(3), pp. 366–374. Available at: https://doi.org/10.7868/s0132342315030082.

Reed, J.L. (1997) 'Electronegativity: Chemical hardness I', *Journal of Physical Chemistry A*, 101(40), pp. 7396–7400. Available at: https://doi.org/10.1021/jp9711050.

Salem, M.A. *et al.* (2018) 'An overview on synthetic strategies to coumarins', *Synthetic Communications*, 48(13), pp. 1534–1550. Available at: https://doi.org/10.1080/00397911.2018.1455873.

Soni, R. *et al.* (2019) 'Design, synthesis and anti-diabetic activity of chromen-2-one derivatives', *Arabian Journal of Chemistry*, 12(5), pp. 701–708. Available at: https://doi.org/https://doi.org/10.1016/j.arabjc.2016.11.011.

Su, C.T.-T., Koh, D.W.-S. and Gan, S.K.-E. (2019) 'Reviewing HIV-1 Gag Mutations in Protease Inhibitors Resistance: Insights for Possible Novel Gag Inhibitor Designs', *Molecules (Basel, Switzerland)*, 24(18), p. 3243. Available at: https://doi.org/10.3390/molecules24183243.

Thomas, V. *et al.* (2017) 'Coumarin Derivatives as Anti-inflammatory and Anticancer Agents.', *Anti-cancer agents in medicinal chemistry*, 17(3), pp. 415–423. Available at: https://doi.org/10.2174/1871520616666160902094739.

Torres, C.F. *et al.* (2014) 'New Insights into the Chemistry and Antioxidant Activity of Coumarins', *Current Topics in Medicinal Chemistry*, pp. 2600–2623. Available at: https://doi.org/http://dx.doi.org/10.2174/1568026614666141203144551.

Tukulula, M., Klein, R. and Kaye, P.T. (2010) 'Indolizine Studies, Part 5: Indolizine-2-carboxamides as Potential HIV-1 Protease Inhibitors[ ]', *Synthetic Communications*, 40(13), pp. 2018–2028. Available at: https://doi.org/10.1080/00397910903219450.

UNAIDS data 2021 (2021). Available at: https://www.unaids.org/en/resources/documents/2021/2021_unaids_data.

Veber, D.F. *et al.* (2002) 'Molecular properties that influence the oral bioavailability of drug candidates', *Journal of Medicinal Chemistry*, 45(12), pp. 2615–2623. Available at: https://doi.org/10.1021/jm020017n.

Zhu, M. *et al.* (2021) 'Design and biological evaluation of cinnamic and phenylpropionic amide derivatives as novel dual inhibitors of HIV-1 protease and reverse transcriptase.', *European journal of medicinal chemistry*, 220, p. 113498. Available at: https://doi.org/10.1016/j.ejmech.2021.113498.